Band Alignment, Built-In Potential, and the Absence of Conductivity at the LaCrO₃/SrTiO₃(001) Heterojunction

S. A. Chambers,[1,*] L. Qiao,[1] T. C. Droubay,[1] T. C. Kaspar,[1] B. W. Arey,[1] and P. V. Sushko[2]

[1]*Pacific Northwest National Laboratory, Richland Washington 99352, USA*
[2]*Department of Physics and Astronomy and London Centre for Nanotechnology, University College London,*
Gower Street, London, WC1E 6BT, United Kingdom
(Received 8 June 2011; published 7 November 2011)

Core-level and valence-band x-ray photoemission spectra measured for molecular-beam-epitaxy-grown $LaCrO_3/SrTiO_3(001)$ yield band offsets and potential gradients within the $LaCrO_3$ sufficient to trigger an electronic reconstruction to alleviate the polarity mismatch. Yet, the interface is insulating. Based on first principles calculations, we attribute this unexpected result to interfacial cation mixing combined with charge redistribution within CrO_2 layers, enabled by low-lying d states within $LaCrO_3$, which suppresses an electronic reconstruction.

The observation of conductivity at the interface of insulating polar and nonpolar perovskites (general form ABO_3) has sparked considerable interest worldwide [1], with much of the work to date being focused on the $LaAlO_3/SrTiO_3(001)$ (LAO/STO) heterojunction [2–4]. Many attribute the interface conductivity to an electronic reconstruction alleviating the polar discontinuity via a film-to-interface charge transfer. However, the possibility of dopant- and/or defect-mediated conductivity cannot be ruled out, especially when the interfaces are not atomically abrupt [5]. Electronic reconstruction requires an electric field within the film to facilitate the charge transfer process. However, x-ray photoemission spectroscopy (XPS) studies reveal little or no electric field in the LAO film either above or below the critical thickness for conductivity (4 u.c.), calling into question the validity of the electronic reconstruction model [5,6]. To broaden this investigation, it is of interest to grow polar perovskites with an alternative metal cation at the B site. Indeed, studies of polar interfaces of $LaMnO_3$ and $LaGaO_3$ [7], as well as $LaVO_3$ [8], with STO(001) prepared by pulsed laser deposition (PLD) have shown that the former is insulating whereas the latter two are conductive above some threshold thickness. Thus, significant unanswered questions remain about the mechanism of conduction at the polar-nonpolar interfaces.

In order to gain deeper insight into the electronic properties, it is worthwhile to manipulate the interface by changing the B-site cation in the polar perovskite. There are no low-lying d—derived bands in LAO. Therefore, if conductivity occurs, it ought to be driven by either the wholesale transfer of charge from the LAO O $2p$-derived band into the STO (i.e. electronic reconstruction), or unintentional doping and/or defect creation. By replacing Al with a transition metal cation, we inject a new degree of freedom into the band structure—partially occupied d orbitals—and, thus, enable other mechanisms of charge redistribution.

In this Letter, we explore this concept by placing Cr(III) at the B site and describe the electronic properties of epitaxial $LaCrO_3$ (LCO)/STO(001) heterojunctions. To minimize defect creation, the films were deposited using molecular beam epitaxy (MBE), in which the incoming atom energies are very low (< 0.1 eV). $LaCrO_3$ (LCO) is an insulator with an optical gap reported to be 3.3 eV [9] for which the experimental electronic properties are well described theoretically with a Hubbard U of zero [10]. Although LCO is orthorhombic in the bulk [11], the pseudocubic lattice parameter for LCO is 3.885 Å, resulting in an excellent lattice match to STO ($a = b = c = 3.905$ Å). According to the electronic reconstruction model, the electrostatic potential in the LCO film should increase with film thickness until the top of the LCO valence band (VB) crosses the bottom of the STO conduction band (CB), giving rise to interface conductivity.

LCO films with La:Cr atom ratios within a few percent of 1.00 were grown by MBE [12]. Band alignment and potential gradients were determined by means of *in situ* high-energy-resolution XPS using a Gamma Data/Scienta SES 200 analyzer with monochromatic Al$K\alpha$ x rays. Conductivity was measured using the van der Pauw method with a specially modified Quantum Design Physical Properties Measurement System designed to measure highly resistive materials [13]. Pt contacts of depth equal to 1 μm were placed at the corners of the films using focused ion beam (FIB) etching and FIB induced deposition of Pt from a methylcyclopentadienyl-trimethyl-platinum precursor, thus allowing conductivity to be detected if it is present in the film, the interface or the substrate. *Ab initio* density functional theory (DFT) calculations were carried out using the PBE and B3LYP functionals, as implemented in the VASP and CRYSTAL packages, respectively, (see Ref. [5] for details).

Figure 1 presents Sr $3d$, La $4d$ and Cr $3p$ core-level spectra as a function of LCO film thickness. All samples
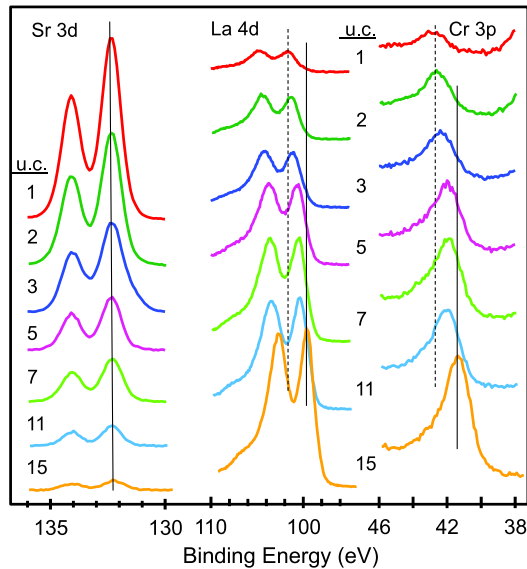
FIG. 1 (color online).   Sr $3d$, La $4d$, and Cr $3p$ spectra for LCO/STO(001) vs film thickness, all measured at an electron take-off angle of 90°. The probe depth is ~5 nm.

FIG. 2 (color online).   Core-level peak widths (a) and potential drop across the film (b) vs. film thickness.

were insulating as judged by XPS, requiring the use of a low-energy electron flood gun to compensate the positive charge. As a result, the binding energy scale is not accurate in an absolute sense. However, with proper flood gun tuning, peak broadening resulting from charging was found to be negligible (< ~0.05 eV) [14]. All spectra in Fig. 1 were shifted to align the Sr $3d_{5/2}$ peaks in order to easily identify trends. There are monotonic decreases in the La $4d$ and Cr $3p$ binding energies, and in the full widths at half maximum (FWHM), with increasing thickness. The drops in Cr and La binding energies reveal an increase in valence-band offset (VBO), as discussed below. The larger FWHM values at small film thicknesses, not seen for LAO/STO [5,6], are attributed to potential gradients across the LCO films.

We show in Fig. 2(a) FWHM values for the La $4d$, Cr $3p$, Sr $3d$ and Ti $2p$ core-level peaks as functions of film thickness. After an increase and plateau up to 11 u.c., the La $4d$ and Cr $3p$ peaks widths decline and converge to a constant value by 15 u.c. Comparison of La $4d$ and Cr $3p$ line shapes for 15, 25, 130, and 260 u.c. films reveals negligible differences in widths [14]. The same is true in comparing the La $4d$ line shape for these films to that of LAO(001). Inasmuch as there are no potential gradients expected within the 130 and 260 u.c. LCO films, or in bulk LAO, this result reveals that the thinner 15 and 25 u.c. films also exhibit a flat-band electronic structure. We estimate the built-in potential in 2–11 u.c. films by modeling the broadened La $4d$ and Cr $3p$ line shapes as sums of appropriately shifted and attenuated spectra from a 25 u.c. film [14]. The results are shown in Fig. 2(b). The built-in potential is ~500 meV/u.c. at 2 u.c. and drops to ~100 meV/u.c. at 11 u.c. There is also some broadening
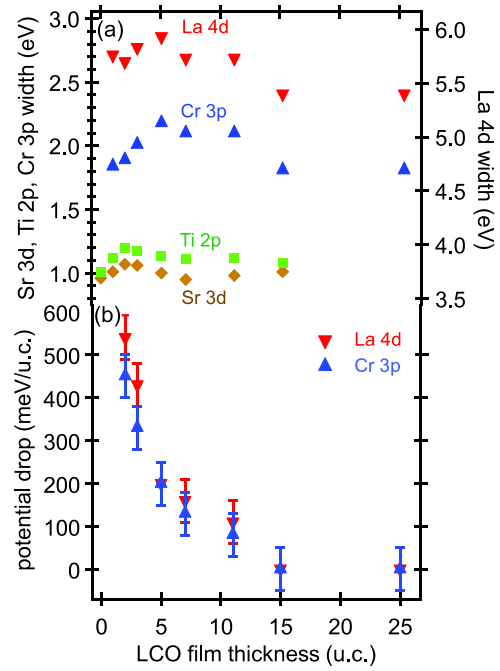
in the STO peaks from 2 to 11 u.c., although it is smaller in magnitude than that observed for La $4d$ and Cr $3p$ [Fig. 2(a)]. Moreover, the broadening is slightly larger for Ti $2p_{3/2}$ than for Sr $3d_{5/2}$. This result may be due to the presence of outdiffused Ti$^{3+\delta}$, as discussed below.

The VBOs (ΔE_v) were determined using core-level binding energies and valence-band maxima (VBM) for LCO/STO(001) heterojunctions and bulk n-STO(001). Pairs of core-level binding energies, one from the substrate and one from the film, were combined with energy differences between the core-level peaks and VBM for bulk STO and thick-film (25 u.c.) LCO to yield VBOs [5]. The analysis was carried out for film thicknesses for which we have adequate sensitivity to both the film and the substrate (2 to 11 u.c.). Sr $3d_{5/2}$ and Ti $2p_{3/2}$ were used for STO, and La $4d$ and Cr $3p$ were used for LCO [14]. The VBOs averaged over all core-level pairs are shown in the lower portion of Fig. 3. The VBO increases from 1.90 (10) eV at 2 u.c. to 2.55(10) eV at 11 u.c.

In order to determine the conduction band offset (CBO or ΔE_c), the band gap of LCO must be known. Based on the strong observed oscillator strength at ~3.3 eV in the optical absorption spectrum for polycrystalline LCO [9], we take this transition to correspond to the O $2p \rightarrow$ Cr $3d$ e_g charge transfer gap. The x-ray excited VB for 25 u.c. LCO/STO(001) (Fig. S6 in Ref. [14]) shows a feature centered at ~1 eV, which B3LYP functional calculations reveal is dominated by Cr $3d$ t_{2g} states with an admixture of O $2p$ character and constitutes the top portion of the VB. The predominantly O $2p$-derived feature is at a binding energy of ~3.2 eV. The energy difference between the
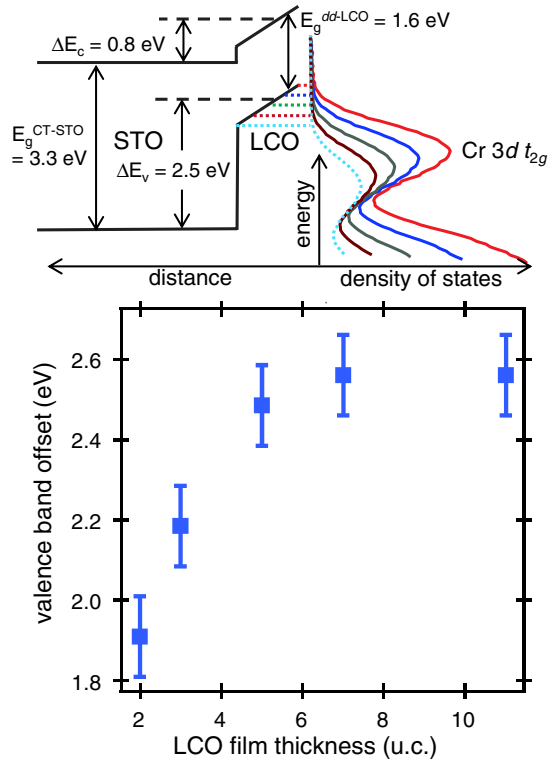
FIG. 3 (color online). (Top) Energy-level diagram illustrating the band offsets and potential gradients extracted from XPS data for 5 u.c. LCO/STO. The five dotted lines in the LCO represent valence-band maxima for each of the u.c. and connect to the associated VB DOS. The dashed lines mark the positions of the intensity-weighted VBM and CBM within the LCO film. (Bottom) Average VBO vs film thickness.

leading edges of the features at ∼1 eV and ∼3.2 eV is 1.7 (1) eV. Thus, the dd (Cr $3d$ $t_{2g} \rightarrow e_g$) gap is ∼$3.3 - 1.7 =$ ∼1.6 eV. The CBO is then estimated to be the VBO plus the Cr $3d$ $t_{2g} \rightarrow e_g$ gap minus the STO band gap (e.g., $\Delta E_c = \Delta E_v + 1.6$–3.3 eV). For all film thicknesses from 2 to 11 u.c., the CBO is positive, which means that the band alignment is staggered (i.e., a type II heterostructure), as depicted in top portion of Fig. 3 for the specific case of 5 u.c. Thus, in all cases, any electronic charge transferred to the STO by an electronic reconstruction should remain within the STO, and the interface should be conductive.

However, the room-temperature (RT) sheet resistances for two patterned 5 u.c. samples were found to be ∼2×10^{13} $\Omega/\square$ and ∼1×10^{8} $\Omega/\square$. The only detected difference between these samples is the La:Cr atom ratio (1.00 in the higher resistivity film and 0.94 in the lower resistivity film). Likewise, two patterned 26 u.c. films each exhibited RT sheet resistances in excess of ∼2×10^{14} $\Omega/\square$. All four samples show insulating or semi-insulating behavior, with sheet resistance values above ∼1×10^{12} $\Omega/\square$ at temperatures below 200 K.

In order to understand the absence of conductivity at LCO/STO(001) interfaces, we consider the electronic

structure calculated for different LCO film thicknesses. One of the candidate mechanisms for reducing the magnitude of the built-in potential is cation intermixing. In the case of LAO/STO, intermixing was shown to decrease the potential drop in the LAO from 270 meV/ Å (for the abrupt interface) to values ranging from ∼90 meV/ Å to ∼0.0 meV/ Å [5] and, at the same time, increase the thermodynamic stability of the interface. We propose that the same effects can play a role in the LCO/STO interface. In particular, we find that for selected configurations, Cr-Ti intermixing gives energy gains of 0.19 and 0.54 eV for LCO thicknesses of 1 and 2 u.c., respectively. We note, however, that these values are markedly smaller than those obtained for equivalent Al-Ti intermixed configurations at the LAO/STO interface: 0.57 and 0.76 eV. This result suggests that cation intermixing in LCO/STO is complemented by a fundamentally different kind of electronic reconstruction—one involving charge redistribution *within* the polar perovskite.

Our thesis is supported by comparative analysis of the layer-projected DOS calculated for atomically abrupt, defect-free LAO/STO and LCO/STO interfaces. For LAO/STO, the top of the O $2p$-derived VB in the LAO shifts to higher energy as the LAO film thickness (N) increases [5]. At $N = 4$ u.c. the LAO VBM becomes iso-energetic with the STO CB minimum and the system becomes metallic. In the case of the LCO/STO interface, the shift of the O $2p$—derived VB is nearly undetectable for $N = 2$, and is at least 3 times less than that in LAO/STO for $N = 4$, as seen in Fig. 4(a). Figure 4(a) also shows that the Cr $3d$ t_{2g} DOS depends significantly on the distance of the Cr atoms from the interface. For $N = 4$, the Cr $3d$ t_{2g} features in the surface CrO_2 layer are ∼1 eV higher in energy and have a very different DOS profile than those in the near-interface CrO_2 layer. In addition, the Cr $3d$ t_{2g} states in the 2nd, 3rd, and 4th u.c. from the interface nearly overlap with Ti $3d$ states in the STO [Fig. 4(a)]. This result
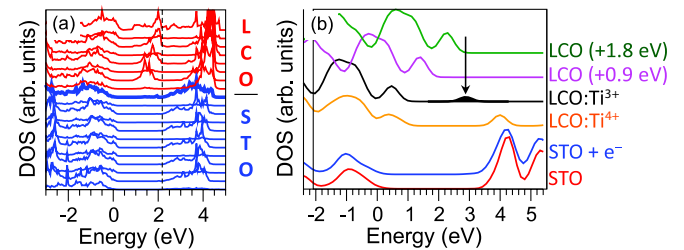

FIG. 4 (color online). (a) DFT PBE densities of states (DOS) projected onto AO and BO_2 atomic planes for an abrupt 4 u.c. LCO/STO(001) interface. The bolded DOS corresponds to the topmost TiO_2 plane. The dashed lines show the position of the Fermi energy when the system is metallic. (b) Embedded-atom B3LYP DOS calculated for STO and LCO containing Ti^{3+} and Ti^{4+} B-site impurities. The peak corresponding to the occupied t_{2g} state of the Ti^{3+} impurity (shown with an arrow) has been scaled by 1.5× for clarity.

points to the possibility of electron transfer within the d states of the B-site atoms, albeit in part owing to PBE severely underestimating the STO band gap. To further investigate this effect, we performed embedded cluster calculations using the B3LYP density functional [14], which well reproduce the STO band gap. Figure 4(b) shows the DOS calculated for STO, LCO, and LCO containing Ti B-site impurities and aligned according to the results of the LCO/STO slab calculations. These DOS suggest that if Ti^{4+} outdiffuses into LCO (for which we have experimental evidence, as seen in Ref. [14]), then Ti^{4+} can trap electrons and produce a localized Ti^{3+} defect state *below* the STO CB minimum. Applying a potential drop of 900 meV/u.c. (a value considered for LAO/STO [6]) to the DOS of each successive LCO unit cell clearly shows that at $N = 3$, a fraction of electron density will be transferred from Cr $3d$ t_{2g} to the Ti^{4+} impurity. Such charge transfer reduces the built-in potential and, in turn, suppresses further cation intermixing. The presence of $Ti^{3+\delta}$ at LCO B sites near the interface may be responsible for the Ti $2p$ peak broadening seen for LCO films up to 11 u.c. in Fig. 2(b).

In summary, we have measured electronic structure properties at MBE-grown LCO/STO(001) interfaces and found evidence for a thickness-dependent potential drop within the LCO film. Although the field magnitude is not as large as expected based on the standard model of a polar film, it is of sufficient magnitude to induce electronic reconstruction and interface conductivity. However, the interface is insulating at LCO film thicknesses large enough to trigger such an electronic reconstruction. Along with the absence of interface conductivity, the weak electric field within the LCO suggests that full-scale electronic reconstruction is suppressed in this system. Electronic structure calculations reveal that, instead, a redistribution of electronic charge within the CrO_2 layers, mediated by outdiffused Ti, occurs. This phenomenon, not previously considered, may be important for understanding and ultimately harnessing for technological purposes the electronic structure of polar-nonpolar interfaces.

*sa.chambers@pnl.gov

[1] A. Ohtomo and H. Y. Hwang, Nature (London) **427**, 423 (2004).
[2] H. H. Chen, A. M. Kolpak, and S. Ismail-Beigi, Adv. Mater. **22**, 2881 (2010).
[3] J. Mannhart and D. G. Schlom, Science **327**, 1607 (2010).
[4] S. A. Chambers, Surf. Sci. **605**, 1133 (2011).
[5] S. A. Chambers, M. H. Engelhard, V. Shutthanandan, Z. Zhu, T. C. Droubay, L. Qiao, P. V. Sushko, T. Feng, H. D. Lee, T. Gustafsson, E. Garfunkel, A. B. Shah, J.-M. Zuo, and Q. M. Ramasse, Surf. Sci. Rep. **65**, 317 (2010).
[6] Y. Segal, J. H. Ngai, J. W. Reiner, F. J. Walker, and C. H. Ahn, Phys. Rev. B **80**, 241107(R) (2009).
[7] P. Perna, D. Maccariello, M. Radovic, U. S. di Uccio, I. Pallecchi, M. Codda, D. Marre, C. Cantoni, J. Gazquez, M. Varela, S. J. Pennycook, and F. M. Granozio, Appl. Phys. Lett. **97**, 152111 (2010).
[8] Y. Hotta, T. Susaki, and H. Y. Hwang, Phys. Rev. Lett. **99**, 236805 (2007).
[9] T. Arima, Y. Tokura, and J. B. Torrance, Phys. Rev. B **48**, 17 006 (1993).
[10] K. P. Ong, P. Blaha, and P. Wu, Phys. Rev. B **77**, 073102 (2008).
[11] J. Yang, Acta Crystallogr. Sect. B **64**, 281 (2008).
[12] L. Qiao, T. C. Droubay, M. E. Bowden, V. Shutthanandan, T. C. Kaspar, and S. A. Chambers, Appl. Phys. Lett. **99**, 061904 (2011).
[13] J. S. McCloy, J. V. Ryan, T. Droubay, T. C. Kaspar, S. Chambers, and D. C. Look, Rev. Sci. Instrum. **81**, 063902 (2010).
[14] See Supplemental Material at http://link.aps.org/supplemental/10.1103/PhysRevLett.107.206802 for the photoelectron spectroscopy and theoretical modeling.